

ABUNDANCES IN GALACTIC H II REGIONS. III. G25.4-0.2, G45.5+0.06, M8, S159, AND DR 22

J. L. PIPHER,^{1, 2} AND H. L. HELFER
 University of Rochester

T. HERTER¹
 Grumman Aerospace Corporation

D. A. BRIOTTA, JR., AND J. R. HOUCK
 Cornell University

S. P. WILLNER²
 Harvard-Smithsonian Center for Astrophysics

AND

B. JONES
 University of California, San Diego
 Received 1983 August 8; accepted 1984 April 4

ABSTRACT

Measurements of the [Ar II] (6.99 μm), [Ar III] (8.99 μm), [Ne II] (12.81 μm), [S III] (18.71 μm), and [S IV] (10.51 μm) lines are presented for five compact H II regions along with continuum spectroscopy. From these data and radio data we deduce lower limits to the elemental abundances of Ar, S, and Ne. G25.4-0.2 is only 6 kpc from the galactic center and is considerably overabundant in all these elements. G45.5+0.06 is 7 kpc from the galactic center and appears to be approximately consistent with solar abundance. S159 in the Perseus arm, 12 kpc from the galactic center, has solar abundance, while M8 in the solar neighborhood may be somewhat overabundant in Ar and Ne. DR 22, 10 kpc from the galactic center in the Cygnus arm, is overabundant in Ar. A summary of results from our series of papers to date on abundances is given.

Subject headings: nebulae: abundances — nebulae: H II regions

I. INTRODUCTION

This is the third paper in a series presenting observations of infrared fine-structure line strengths in galactic H II regions for the purpose of assessing abundances in the Galaxy. Hereafter Paper I and Paper II are used to refer to Herter *et al.* 1981 and 1982*b*, respectively. As we have pointed out before, infrared observations allow one to probe large distances from the Sun or deep within a molecular cloud, although substantial extinction corrections are required in these cases. The weak temperature dependence of the line strengths and the potential for obtaining data on two important ionization states of the argon and sulfur atoms allow direct abundance analysis using the infrared lines.

In this paper we report ground-based and airborne spectroscopic fine-structure line observations from 2 to 30 μm for the compact H II region complexes of G25.4-0.2, G45.5+0.06, M8, S159, and DR 22. The regions G25.4-0.2 and G45.5+0.06 are near the regions G29.9-0.0 and G45.1+0.1 studied in Paper I. G25.4-0.2, at 5.5 kpc, is the closest H II region to the galactic center studied in this series. The region M8 has been extensively studied at optical wavelengths, allowing direct comparison of infrared and optical abundance estimates. DR 22 is near S106, studied in Paper II, and S159 is another example of a Perseus arm H II region (S158 and S156

were studied in Papers I and II, respectively). Since Talent and Dufour (1979) have suggested the existence of substantial abundance gradients along the Perseus arm, these last H II regions are of particular interest.

The fine-structure lines studied here include the [Ar III] and [Ar II] lines at 8.99 μm and 6.99 μm ; the [S III] and [S IV] lines at 18.71 μm and 10.51 μm ; and the [Ne II] line at 12.81 μm . These argon and sulfur ionization states constitute the major ionization states for H II regions with exciting stars of temperature $T_* = 30,000$ –45,000 K for sulfur and $T_* = 25,000$ –40,000 K for argon according to simple dust-free ionization structure models (e.g., Lacasse *et al.* 1980, Lacy 1981). The ionic fraction of Ne II is expected to be strongly correlated with the ratio S III/S IV (see Herter, Helfer, and Pipher 1983), so that total atomic abundances of argon, sulfur, and neon can be obtained from these observations.

In § II we present the observational techniques employed, and a brief review of the methods outlined in Papers I and II for estimating and applying extinction corrections and determining ionic and elemental abundances. Individual source data and subsequent abundance estimates are given in § III, and a summary of the abundances from the present work and Papers I and II is presented in § IV.

II. OBSERVATIONS

The data described here were obtained with a variety of infrared systems. Ground-based data were obtained primarily at the Kitt Peak National Observatory (KPNO), Cerro Tololo Inter-American Observatory (CTIO), or the University of California, San Diego–University of Minnesota Mount Lemmon

¹ Visiting Astronomer, Kitt Peak National Observatory, Tucson, Arizona, which is operated by the Associated Universities for Research in Astronomy, Inc., under contract with the National Science Foundation.

² Visiting Astronomer, Cerro Tololo Inter-American Observatory, La Serena, Chile. Operated by the Associated Universities for Research in Astronomy, Inc., under contract with the National Science Foundation.

Observatory using CVF spectrometers with resolutions of $\Delta\lambda/\lambda \sim 0.015$. These data, both previously published and new results, are noted in Table 1. Sampling densities are typically one to two data points per resolution element. Chopper spacings employed for each object are given in § IIIc.

The 4–8 μm data reported here consist of observations in the [Ar II] line and adjacent continuum using the UCSD filter-wheel spectrometer with a resolution $\lambda/\Delta\lambda$ of 0.015 (Russell, Soifer, and Willner 1977; Puetter *et al.* 1979) on flights of the Kuiper Airborne Observatory (KAO) in 1980 July and 1981 June and August. For these observations a 27" focal plane aperture was employed, and chopped beam spacing and orientation were chosen to avoid beam cancellation.

The [S III] 18.71 μm line fluxes of G25.4–0.2, S159, and G45.5+0.06 were obtained with a 10 channel cooled-grating spectrometer (McCarthy, Forrest, and Houck 1979) in 1980 July. A focal plane aperture of 30" was used, and the spectral resolution was approximately 0.2 μm . Observations of the [S III] lines of M8 and DR 22 were made with a three channel cooled-grating spectrometer (Herter *et al.* 1982a) in 1981 August. The focal plane aperture was approximately 20", and the spectral resolution was 0.033 μm . For both sets of observations the choice of beam throw was similar to that used with the UCSD instrument.

The observed line fluxes (uncorrected for extinction) are listed in Table 1 along with the beam sizes. The line fluxes for all but [Ar II] have been derived from a least squares fit to the observations of the form $F_\lambda = a + b\lambda + c\{\exp[-(\lambda$

$-\lambda_c)/\sigma_\lambda]^2\}$, that is a linear continuum plus unresolved line emission at $\lambda = \lambda_c$, and $\sigma_\lambda \sim 0.6\Delta\lambda_{\text{FWHM}}$, where $\Delta\lambda_{\text{FWHM}}$ was determined from laboratory measurements. We vary a, b, c to minimize $\chi^2 = \Sigma[(F_{\text{obs}} - F_{\text{model}})/\text{obs. error}]^2$. For [Ar II] only one point in the line and one on either side in the adjacent continuum were used to estimate the line flux.

III. DISCUSSION

a) Estimating Extinction

In Paper I we extensively discussed the nature of the extinction correction, and here we will only briefly review the correction techniques and the uncertainties involved. The extinction can be computed from the brightness of the hydrogen emission lines or from the depth of the 9.7 μm silicate absorption. In the former method, we can accurately compute the extinction at 2.17 μm and 4.05 μm by comparing observed and predicted Brackett-line fluxes with the free-free radio flux density or by comparing the observed and predicted ratio of the Brackett-line fluxes and assuming the form of the extinction law from 2 to 4 μm . However, the short-wavelength extinction cannot be easily extrapolated to the longer wavelengths at which the fine-structure lines appear. Alternatively, the 9.7 μm silicate extinction (Gillett *et al.* 1975) can be determined by fitting the absorption spectrum of the 8–13 μm continuum radiation with an opacity law τ_λ which fits the optically thin emission from hot dust in the Trapezium. For some sources, unidentified emission features at 7.7, 8.6, and 11.3 μm strongly affect the

TABLE 1
OBSERVED AND EXTINCTION-CORRECTED LINE FLUXES

Object	$\bar{\tau}_{9.7}$	Line	Beam (")	Flux ^a ($10^{-18} \text{ W cm}^{-2}$)	τ_λ	Corrected Flux ($10^{-18} \text{ W cm}^{-2}$)
G25.4–0.2	5.3 ± 0.3	Ar II	27	4.0 ± 0.5	1.6 ± 0.1	20 ± 4
		Ar III	15	<0.4	4.2 ± 0.2	<27
		S III	30	5.0 ± 1.4	3.2 ± 0.2	123 ± 42
		S IV	15	<0.5	4.5 ± 0.3	<45
		Ne II	15	20 ± 2	1.9 ± 0.1	130 ± 20
G45.5+0.06	2.8 ± 0.4	Ar II	27	4 ± 2	0.8 ± 0.1	8.7 ± 4
		Ar III	15	1.8 ± 0.3	2.2 ± 0.3	16 ± 6
		S III	30	16 ± 1.5	1.7 ± 0.2	88 ± 19
		S IV	15	2.6 ± 0.4	2.4 ± 0.3	29 ± 10
		Ne II	15	12 ± 1	1.0 ± 0.1	33 ± 4
M8	0.0	Ar II	27	10 ± 2.5	0.0	10 ± 2.5
		Ar III	15	2.3 ± 0.3		2.3 ± 0.3
		S III	20	26 ± 1		26 ± 1
		S IV	15	<1.2		<1.2
		Ne II	15	23 ± 2		23 ± 2
		Br γ	9	0.23 ± 0.01		0.23 ± 0.01
S159	0.0	Ar II	27	4.2 ± 0.8	0.0	4.2 ± 0.8
		Ar III	22	<1.4		<1.4
		S III	30	12 ± 1.3		12 ± 1.3
		S IV	22	<1.7		<1.7
		Ne II	22	20 ± 1		20 ± 1
DR 22	2.2 ± 0.3	Ar II	27	10.7 ± 3	0.7 ± 0.1	21.5 ± 7
		Ar III	11	0.8 ± 0.2 ^b	1.8 ± 0.2	4.8 ± 1.6
		S III	20	17 ± 1	1.3 ± 0.2	62 ± 13
		S IV	11	<1.2 ^b	1.9 ± 0.3	<8
		Ne II	11	7.1 ± 1.0 ^b	0.8 ± 0.1	16 ± 3
		Br γ	11	0.12 ± 0.01 ^b	2.25 ± 0.3	1.14 ± 0.15
		Br α	11	0.97 ± 0.04 ^b	1.20 ± 0.15	3.22 ± 0.4

^a Uncorrected for extinction.

^b Measurements at peak radio flux position.

TABLE 2
 DETERMINATION OF IONIC ABUNDANCES

Object	Line	S_ν (Jy)	$j/n_x^i n_e$ (10^{-22} ergs $\text{cm}^3 \text{s}^{-1} \text{sr}^{-1}$)	n_x^i/n_{H} (10^{-6})	(n_x^i/n_{H}) (with respect to standard atomic abundance) ^a
G25.4-0.2	Ar II	2.5	3.14	9.0 ± 1.8	1.9 ± 0.4
	Ar III	2.0	7.24	<6.6	<1.4
	S III	2.5	5.82	30 ± 10	1.8 ± 0.6
	S IV	2.0	25.94	<3.06	<0.2
	Ne II	2.0	0.940	243 ± 30	2.4 ± 0.2
G45.5+0.06	Ar II	3.3	3.16	2.9 ± 1.5	0.6 ± 0.3
	Ar III	3.3	7.46	2.3 ± 0.9	0.5 ± 0.2
	S III	3.3	7.67	12 ± 2	0.8 ± 0.2
	S IV	3.3	30.19	1.0 ± 0.4	0.06 ± 0.02
	Ne II	3.3	0.961	37 ± 4	0.36 ± 0.03
M8	Ar II	1.91	3.16	6.4 ± 1.6	1.4 ± 0.4
	Ar III	0.67	7.46	1.8 ± 0.2	0.38 ± 0.05
	S III	1.24	7.93	10.2 ± 0.4	0.64 ± 0.24
	S IV	0.67	31.16	<0.25	<0.02
	Ne II	0.67	0.961	43 ± 13	1.39 ± 0.08
S159	Ar II	1	3.14	4.7 ± 0.9	1.0 ± 0.2
	Ar III	1	7.24	<0.7	<0.2
	S III	1	5.82	7.5 ± 0.7	0.46 ± 0.05
	S IV	1	25.94	<0.25	<0.01
	Ne II	1	0.940	75 ± 4	0.75 ± 0.03
DR 22	Ar II	3.2	3.17	7.0 ± 2	1.5 ± 0.4
	Ar III	1.1 ^b	7.59	2.2 ± 0.5	0.46 ± 0.10
	S III	3.2 ^c	9.32	6.6 ± 1.7	0.42 ± 0.09
	S IV	1.1 ^b	33.33	<0.9	<0.06
	Ne II	1.1 ^b	0.973	60 ± 6	0.60 ± 0.06

^a Assumed standard abundances: S/H = 1.6×10^{-5} ; Ar/H = 4.7×10^{-6} ; Ne/H = 1.0×10^{-4} .

^b Deduced from Br γ flux corrected for extinction.

^c $\nu = 10.7$ GHz.

spectrum. For these sources, a multicomponent fit of the form developed by Aitken *et al.* (1979) and Jones *et al.* (1980) is used to provide a better estimate of $\tau_{9.7}$.

For each source, all of the available techniques have been used to estimate the extinction. A single extinction law, given in Paper I, was used, although there is no guarantee that the extinction law is the same from region to region. The extinctions derived from the different techniques were converted to values of $\tau_{9.7}$, and the mean was computed for each source. The means $\bar{\tau}_{9.7}$ are listed in Table 1, along with their uncertainties. The stated uncertainties in the corrected line fluxes and calculated abundances include the estimated uncertainty in the adopted $\bar{\tau}_{9.7}$.

b) Estimating Abundances

Ionic abundances were estimated by comparison of the corrected line fluxes with radio flux densities, measured at wavelengths short enough that the nebulae are optically thin (eq. [3], Paper I). The electron temperature was assumed to be 7500 K, and the ratio of electrons to protons, 1.15. The electron density was estimated from the radio flux density and source size with an assumed filling factor of 1. New, more reliable and accurate values of the sulfur collision strengths have been employed (Mendoza 1983) in computation of the ionic abundances, listed in Table 2. Table 3 lists the revised S III and S IV abundances (using the new collision strengths) for objects studied in Papers I and II.

The prescription for computing total atomic abundances for argon and sulfur from the [Ar II], [Ar III], [S III], and [S IV]

observations was discussed in Paper I. The abundances thus computed, and displayed in Figures 1-4, are strictly lower limits to the total abundance because (1) other ionization states may be present, (2) clumping may cause us to underestimate ionic abundances, and (3) sources extended with respect to measurement beam sizes lead to exclusion of certain ionic contributions, as discussed in Paper I.

 TABLE 3
 REVISED SULFUR IONIC ABUNDANCES $(n_x^i/n_{\text{H}})/(n_x^i/n_{\text{H}})_{\text{standard}}$
 FOR OBJECTS FROM PAPERS I AND II

Source	S IV	S III	Galactocentric Radius R (kpc)
Paper I			
G29.9-0.0	<0.06	1.0 ± 0.39	5
G12.8-0.2	0.04 ± 0.01	0.22 ± 0.05	6
G45.1+0.1	0.08 ± 0.03	0.37 ± 0.08	7.5
G75.84+0.4	0.06 ± 0.006	1.21 ± 0.06	10
W3 IRS 1	0.14 ± 0.04	0.67 ± 0.12	12
NGC 7538 IRS 2	0.01 ± 0.02	0.34 ± 0.17	12.7
Paper II			
S88B	<0.07	0.48 ± 0.34	9
S156	1.00 ± 0.18	11.7
S106	<0.04	0.68 ± 0.14	10
NGC 2170 IRS 1	<0.01	0.27 ± 0.07	12.5
M42 (20°N θ , C)	0.09 ± 0.01	0.61 ± 0.06	10.5

NOTE.—Revised abundances using the collision strengths of sulfur from Mendoza 1983.

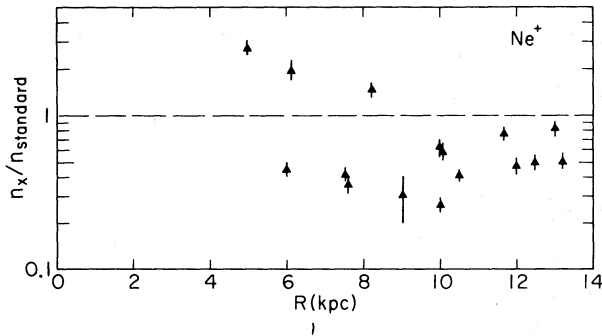


FIG. 1.—Ratio of $n_x/n_{\text{standard}} = (\text{Ne}^+/\text{H})/(\text{Ne}/\text{H})_{\text{standard}}$ as a function of galactocentric radius R ; $12 + \log (\text{Ne}/\text{H})_{\text{standard}} = 8.0$.

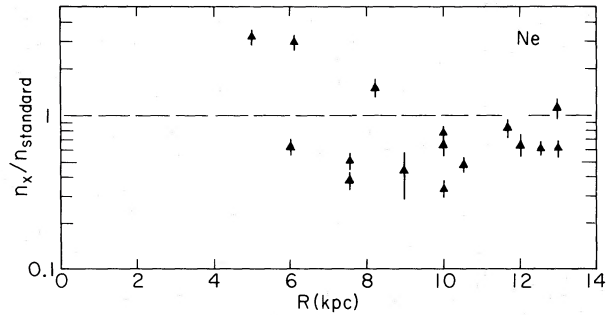


FIG. 2.—Ratio of $n_x/n_{\text{standard}} = (\text{Ne}/\text{H})/(\text{Ne}/\text{H})_{\text{standard}}$ as a function of galactocentric radius R ; $12 + \log (\text{Ne}/\text{H})_{\text{standard}} = 8.0$.

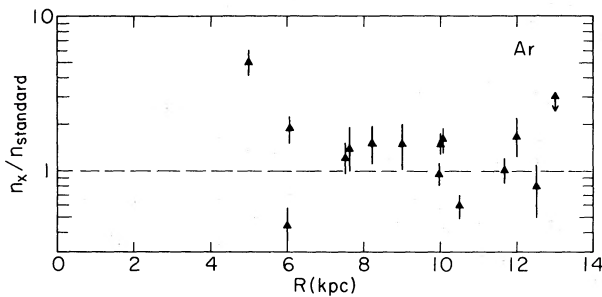


FIG. 3.—Ratio of $n_x/n_{\text{standard}} = (\text{Ar}/\text{H})/(\text{Ar}/\text{H})_{\text{standard}}$ as a function of galactocentric radius R ; $12 + \log (\text{Ar}/\text{H})_{\text{standard}} = 6.67$.

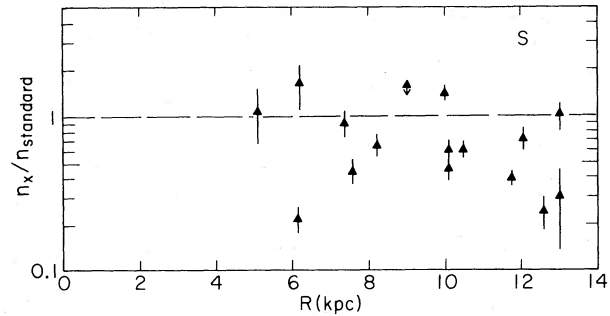


FIG. 4.—Ratio of $n_x/n_{\text{standard}} = (\text{S}/\text{H})/(\text{S}/\text{H})_{\text{standard}}$ as a function of galactocentric radius R ; $12 + \log (\text{S}/\text{H})_{\text{standard}} = 7.20$.

Since only one ionization state of neon was observed (Ne II), it is more difficult to calculate the total neon abundance. However, in spherical, uniform models of H II regions employing the OTS (On the Spot) approximation with charge exchange included, under the assumption of uniform temperature, it is found that the ionic fraction of $\text{Ne II}/\text{Ne}$ is correlated with the ratio $\text{S III}/\text{S IV}$, so that the total neon abundance can also be estimated from the Ne II measurement (Herter, Helfer, and Pipher 1983).

The mean electron density, distance, and galactocentric radius for each region are given in Table 4.

c) Individual Sources

i) G25.4-0.2 = W42

Radio maps of the G25.4-0.2 region show two sources; the one we studied³ has a half-power diameter of 10" and total diameter 20" (Herter and Krassner 1984). The kinematic distance is 4.7 ± 0.7 kpc (Reifenstein *et al.* 1970). It is situated near

³ $\alpha_{1950} = 18^{\text{h}}35^{\text{m}}26^{\text{s}}5$, $\delta_{1950} = -06^{\circ}48'38''$ (Herter and Krassner 1984).

overabundant H II regions G29.9-0.0 and G30.8-0.0 (Paper I; Lester *et al.* 1981), which are also within 6 kpc of the galactic center. Felli, Tofani, and D'Addario (1974) give a 10.7 GHz radio flux density for this component of 2.5 Jy; Herter and Krassner (1984) observed the source on the VLA at 5 GHz and confirm the flux density of Felli *et al.* Observations of the 8-13 μm spectrum of G25.4-0.2 were obtained on the KPNO 2.1 m telescope in 1980 June with a beam throw of 25" and a 14"8 aperture, which included 80% of the radio flux. A model II fit to the very deep silicate feature in the 8-13 μm spectrum gives $\tau_{9.7} = 5.3 \pm 0.3$, and the only fine-structure line observed was the $[\text{Ne II}]$ line. Observations of the $[\text{S III}]$ and $[\text{Ar II}]$ lines were obtained in 1980 July and 1981 June on the KAO, with a 2' beam throw. Abundances were computed assuming $S_{\nu} = 2.5$ Jy for the $[\text{Ar II}]$ and $[\text{S III}]$ lines, and $S_{\nu} = 2.0$ Jy for the $[\text{Ne II}]$ line (measured with a smaller beam).

ii) G45.5+0.06

G45.5+0.06 has been extensively studied in the radio and infrared. Zeilik, Kleinmann, and Wright (1975) mapped this compact H II region at 10.6 μm and also presented photo-

TABLE 4
ASSUMED PHYSICAL PARAMETERS OF OBSERVED OBJECTS

Objects	n_e^{rms} (cm^{-3})	Distance d (kpc)	Galactocentric Radius R (kpc)
G25.4-0.2	10^4	4.7 ± 0.7 (13.4 ± 0.7)	6.1
		[near and far distances]	
G45.5+0.06, component A	5800	9.7	7.6
M8 (in a 9" beam)	5000	1.8	8.2
S159A	10^4	4.5	11.7
DR 22	3400	3.4 ± 1.8	10

metry; in addition, Zeilik and Heckert (1977) mapped the region at $2.2 \mu\text{m}$ with a large beam ($1'$). Radio maps by Wynn-Williams, Downes, and Wilson (1971) Matthews *et al.* (1977) at 5 GHz with a resolution of $7'' \times 35''$ reveal that G45.5+0.06 consists of three components: a $13''$ diameter source, A, of 3.3 Jy radio flux density, and two more diffuse low-density components, B and C, of $26''$ and $100''$, respectively. At an adopted kinematic distance of 9.7 kpc (Reifenstein *et al.* 1970), Matthews *et al.* conclude that a 47,000 K zero-age main-sequence exciting star is necessary to ionize component A.

The 8–13 μm spectrum, obtained with a $14''.8$ aperture and a $28''$ beam throw at the KPNO 2.1 m telescope in 1980 June, was taken by offsetting to radio position A of Matthews *et al.* and peaking up on the [Ne II] flux. All three fine-structure lines available in this wavelength range are present. There is some indication that the unidentified 11.3 μm emission feature may be present. The substantial silicate extinction is reproduced by a model II fit with $\tau_{9.7} = 3.1$, or a multicomponent fit of 2.6 if graphite grains are present, and 3.0 if they are not. We adopt $\tau_{9.7} = 2.8 \pm 0.4$, since we do not have 2–4 μm data on this source.

The [S III] and [Ar II] line flux measurements were obtained on the KAO in 1980 June and 1981 July, respectively, with beam throws of $2'$.

Ionic abundances were computed from the corrected line fluxes assuming that component A is the major contributor to the ionized gas. Any contribution from other, more diffuse components should have been canceled out by chopping.

iii) M8

M8 and the surrounding region constitute one of the most extensively studied H II region/molecular cloud complexes. In the vicinity there are a young cluster (NGC 6530), the Hourglass bright optical H II region, and more extended diffuse optical emission. While 9 Sgr is thought to power much of the optical nebulosity, the O7 star Herschel 36 may power the nearby Hourglass (Thackeray 1950; Woolf 1961). Maps at radio wavelengths show that the radio center coincides with the northern lobe of the Hourglass (Turner *et al.* 1974; Wink, Altenhoff, and Webster 1975): a high-resolution VLA map at 5 GHz (Woodward *et al.* 1984) is used in the analysis below. Infrared maps by Dyck (1977), Wright *et al.* (1977), Zeilik (1979), Thronson, Loewenstein, and Stokes (1979), and Woodward *et al.* (1984) show peaks at or near the northern Hourglass/Herschel 36 region. An 8–13 μm spectrum centered on the narrow "waist" of the Hourglass was obtained on the KPNO 2.1 m telescope in a $15''$ aperture with a $60''$ beam throw in 1980 June, and a partial 2–4 μm spectrum was obtained on the CTIO 1.5 m telescope in 1980 July in a $9''$ aperture, with a $30''$ beam throw. Observations of the [Ar II] and [S III] lines were obtained at KAO in 1981 June and August. The extinction to M8 has been estimated by a multicomponent fit to the 8–13 μm spectrum as $\tau_{9.7} = 0$. This is in excellent agreement with the visual estimate to the Hourglass of $A_v = 2.4$ assuming Orion-type selective extinction or $A_v = 1.1$ assuming standard selective extinction (Johnson 1967). Lynds and O'Neil (1982) find $A_v = 3.6$ assuming a standard extinction law. We cannot reliably estimate the extinction from the Br γ flux and VLA radio map since there is evidence of a possible compact source with partially optically thick Brackett lines in the beam. Hence, the corrected line fluxes are taken to be equal to the observed line fluxes. Ionic abundances are computed using the 5 GHz VLA radio flux density estimated for the appropriate beam size (Woodward *et al.* 1984).

iv) S159A = AFGL 3053

S159A was included in the 5 GHz aperture synthesis observations of Perseus arm H II regions by Israel (1977). The radio diameter of the compact component is $6''$, and the optically thin 5 GHz density is 1.0 Jy. Rossano and Russell (1981) found an extended component as well; in a $4'.5$ beam at 3.2 GHz, the radio flux density is 2.43 Jy. An exciting star of $\sim 35,000$ K is required to support the radio emission; hence, S159A is a fairly low excitation compact H II region. S159A is near a peak in the CO emission and is at the position of an optically bright wisp, as noted by Israel. The 8–13 μm spectrum of AFGL 3053 was obtained by Merrill (1977) with a $17''$ beam and a $50''$ beam throw at Mount Lemmon in 1976 December; that spectrum shows a substantial [Ne II] line as well as very strong 8.6 and 11.3 μm unidentified emission features. The [Ar II] and [S III] measurements were obtained on KAO in 1981 June and 1980 July, respectively.

Because 8.6 μm and 11.3 μm features dominate the 8–13 μm spectrum, it is necessary to use a multicomponent fit to estimate the extinction. We conclude on the basis of the fit that $\tau_{9.7} = 0$ and list the corrected line fluxes equal to the measured line fluxes in Table 1.

Ionic abundances are computed assuming $S_v = 1.0$ Jy.

v) DR 22

DR 22 is one of the 27 sources found in a 5 GHz survey of the Cygnus X complex by Downes and Rinehart (1966). Felli, Tofani, and D'Addario (1974) found DR 22 to be $\sim 16''$ in size with a 10.7 GHz radio flux density of 3.2 Jy. High-resolution radio maps of DR 22 at 2.7 GHz (Krassner *et al.* 1983) and on the VLA at 5 GHz (Herter and Krassner 1984) yield a size of $22''$, and the radio flux density can be supported by an exciting star of $\sim 37,000$ K. The 2–4 and 8–13 μm spectra of DR 22 were obtained with an $11''$ aperture with a $53''$ NS beam throw at the radio peak by Herter (1984), and the [Ar II] and [S III] data were obtained in 1981 June and August. Herter (1984) mapped DR 22 in the Brackett lines and adjacent continua with an $11''$ beam and found the extinction in the nebula varied from $\tau_{\text{Br}\gamma} = 1.4$ to 2.7. He deduced that the abundance of [Ne II] is remarkably constant with position in the nebula. The radio flux density used in the abundance analyses of [Ne II], [Ar III], and [S IV] is 1.1 Jy derived from the extinction-corrected Br γ and Br α fluxes.

IV. ABUNDANCES

We give the ionic abundances computed for each source in Table 2. G25.4–0.2, 6.1 kpc from the galactic center, is overabundant in Ar II, S III, and Ne II. Since the half-power size of G25.4–0.2 is smaller than our measurement beam sizes, we can simply add ionic abundances of argon and sulfur to obtain atomic abundances. Because [Ar III] and [S IV] were not detected, we take the Ar II and S III abundances to be equal to the atomic abundances. Since S III/S IV > 9 , we estimate that Ne II constitutes $\sim 90\%$ of the neon in the nebula (Herter, Helfer, and Pipher 1983). Thus neon is 2.4–2.7 times standard. Hence G25.4–0.2, like G29.9–0.0, is overabundant compared with standard abundances by approximately a factor of 2.

Similarly, G45.5+0.06, at 7 kpc, is also small compared with our measurement beam sizes. We find total abundances of argon and sulfur to be 1.1 and 0.86 times standard abundances, respectively. Since the ratio of S III/S IV is 13, indicating a *much* softer UV radiation field than that of the single 47,000 K star required to support the observed radio flux density, we con-

clude that most of the neon is Ne II, and that the neon abundance is only 0.4 times standard abundance.

S159, a member of the Perseus arm, is 12 kpc from the galactic center and is also small compared with our measurement beam sizes. It is a low-excitation H II region, and most of the argon, sulfur, and neon is in the Ar II, S III, and Ne II ionic states. Hence, atomic abundances of 1, 0.5, and 0.8 are deduced for argon, sulfur, and neon, respectively; i.e., we find S159 to have approximately standard abundances of these elements.

Both M8 and DR 22 are extended with respect to our measurement beams and are 8.2 and 10 kpc from the galactic center, respectively. Both M8 and DR 22 have been studied in the radio at high resolution by Woodward *et al.* (1984) and Herter (1984), and these maps are used to compute total Ar and S abundances using the techniques discussed in Paper I. Maps in the [Ne II] lines and studies of the extinction have been made for DR 22 (Herter 1984). We estimate the atomic abundances of Ne and S in DR 22 to be consistent with standard abundances, while DR 22 is slightly overabundant in Ar. M8 is apparently overabundant in Ne and Ar.

In Figures 1–4 we have plotted the estimated atomic abundances of Ar, S, and Ne, as well as Ne⁺, as compared with solar abundance for the sixteen H II regions we have studied in Papers I, II, and the present paper, assuming no uncertainty in R , the galactocentric distance. In these figures, the Ne⁺ abundances from Paper I have been adjusted to reflect the standard neon abundance used in Paper II, and these abundances have been converted to total neon abundances using the observed [S III/S IV] ratios. Despite the fact that there is scatter about the solar abundance value, we immediately can conclude there is no compelling observational evidence for extreme abundance gradients in our Galaxy in these three elements. While there is a slight trend toward decreasing abundance with increasing galactocentric radius R , the result depends heavily on the few observations obtained to date at $R \leq 6$ kpc. The formal results for argon, neon, and sulfur are $d \log (\text{Ar}/\text{H})/dR = -0.06 \text{ kpc}^{-1}$, $d \log (\text{Ne}/\text{H})/dR = -0.19 \text{ kpc}^{-1}$, and $d \log (\text{S}/\text{H})/dR = -0.10 \text{ kpc}^{-1}$, respectively. These should be compared with O/H and N/H results from 8 to 14 kpc in the solar neighborhood obtained by Peimbert, Torres-Peimbert, and Rayo (1978), who quote gradients, in the same units, of -0.13 and -0.23 , respectively. A recent paper by Shaver *et al.* (1983), using combined optical and radio observations, cites oxygen and nitrogen gradients of -0.07 and -0.09 , in the same units, with very small scatter. Their results for other elements are less certain because of observational difficulties, but they suggest that sulfur may have a much smaller gradient. The scatter in the present results is larger than they found for O and N. Talent and Dufour (1979) have derived substantial abundance gradients with galactocentric distance along a given spiral arm using optical measurements: these determinations exhibit much less scatter than the global studies (both optical and infrared). We have not yet obtained a sufficient infrared sample along a spiral arm to assess these findings.

We must draw attention to W33 (G12.8–0.2), the low point

at 6 kpc on all four figures. The argon and sulfur measurements lead to the conclusion that W33 is underabundant compared with standard. However, a previous large-beam measurement in S III showed it to be overabundant (McCarthy 1980; see Paper I). A second small-beam (20") measurement in S III with chopper throws of 5' and 6' oriented NE to SW yielded results identical to those of Paper I (T. H.). A possible explanation of the small-beam S III measurements is that high-density clumps exist in the region: if so, the S III abundance is underestimated. Further plans include measurement of the [S III] 33 μm line to estimate the density. Aperture synthesis maps of W33 recently published (Ho and Haschick 1981) may help future detailed studies of the region.

V. CONCLUSION

Abundance measurements for a total of 16 H II regions based on Ar, Ne, and S infrared fine-structure lines show a slight trend toward decreasing abundances with increasing galactocentric radius. Region-to-region scatter at nearly constant radius is, however, as large as the alleged gradient. In particular, we measure low abundances for W33 at small radius, while S158 and S106 have high abundances at larger radii. The latter determinations seem secure, while the determination for W33 is less so.

The major uncertainties in abundance measurements in the infrared include (1) beam size corrections, (2) extinction corrections, and (3) corrections for unmeasured ionization states. The first two of these might potentially explain the low abundances derived for W33. As noted in § IV, the presence of high-density clumps can dramatically affect the S III emissivity, so that the S abundance would be underestimated (see Herter *et al.* 1982a). It is imperative that both ionization states of argon and sulfur be measured with the same large (with respect to source diameter) beam size if uncertainties due to item 1 are to be ruled out: an alternative method would be complete maps in the lines. Also, if a greater number of hydrogen recombination lines were measured in each region in order to tie down the extinction law, and hence the appropriate extinction for each fine-structure line, *with the same large beam*, the second uncertainty could be alleviated. Finally, empirical relationships concerning the excitation conditions or correction for the unmeasured ionization states are required. The total neon abundance has been estimated here from a model correlation between the Ne II fraction and the [S III/S IV] ratio, for example.

In spite of the uncertainties, there appear to be real differences among the abundances for different elements. There also appears to be a real spread in element abundances, at least at a galactocentric radius near that of the Sun.

It is a pleasure to acknowledge the superlative support staffs at KAO, CTIO, and KPNO. We thank G. Gull and M. Shure for assistance with the measurements and equipment development. All the authors have been supported in this work by grants from NASA.

REFERENCES

- Aitken, D. K., Roche, P. F., Spenser, P. M., and Jones, B. 1979, *Ap. J.*, **233**, 60.
 Downes, D., and Rinehart, R. 1966, *Ap. J.*, **144**, 937.
 Dyck, H. M. 1977, *A. J.*, **82**, 129.
 Felli, M., Tofani, G., and D'Addario, L. R. 1974, *Astr. Ap.*, **31**, 431.
 Gillett, F. C., Forrest, W. J., Merrill, K. M., Capps, R. W., and Soifer, B. T. 1975, *Ap. J.*, **200**, 609.
 Herter, T. 1984, in preparation.
 Herter, T., *et al.* 1981, *Ap. J.*, **250**, 186 (Paper I).
 Herter, T., Briotta, D. A., Jr., Gull, G. E., Shure, M. A., and Houck, J. R. 1982a, *Ap. J. (Letters)*, **259**, L25.
 Herter, T., Helfer, H. L., and Pipher, J. L. 1983, *Astr. Ap. Suppl.*, **51**, 195.
 Herter, T., Helfer, H. L., Pipher, J. L., Briotta, D. A., Jr., Forrest, W. J., Houck, J. R., Rudy, R. J., and Willner, S. P. 1982b, *Ap. J.*, **262**, 153 (Paper II).
 Herter, T., and Krassner, J. 1984, in preparation.

- Ho, P. T. P., and Haschick, A. D. 1981, *Ap. J.*, **248**, 622.
 Israel, F. P. 1977, *Astr. Ap.*, **59**, 27.
 Johnson, H. L. 1967, *Ap. J.*, **147**, 912.
 Jones, B., Merrill, K. M., Stein, W., and Willner, S. P. 1980, *Ap. J.*, **242**, 141.
 Krassner, J., Pipher, J. L., Savedoff, M. P., and Soifer, B. T. 1983, *A.J.*, **88**, 972.
 Lacasse, M. G., Herter, T., Krassner, J., Helfer, H. L., and Pipher, J. L. 1980, *Astr. Ap.*, **86**, 231.
 Lacy, J. 1981, in *IAU Symposium 96, Infrared Astronomy*, ed. C. G. Wynn-Williams and D. P. Cruikshank (Dordrecht: Reidel), p. 237.
 Lester, D., Dinerstein, H., Werner, M., Watson, D., Genzel, R., Townes, C., Storey, J., and Harvey, P. 1981, *Bull. AAS*, **13**, 808.
 Lynds, B. T., and O'Neil, E. J., Jr. 1982, *Ap. J.*, **263**, 130.
 Matthews, H. E., Goss, W. M., Winnberg, A., and Habing, H. J. 1977, *Astr. Ap.*, **61**, 261.
 McCarthy, J. F. 1980, Ph.D. thesis, Cornell University.
 McCarthy, J. F., Forrest, W. J., and Houck, J. R. 1979, *Ap. J.*, **233**, 611.
 Mendoza, C. 1983, in *IAU Symposium 103, Planetary Nebulae*, ed. D. R. Flower (Dordrecht: Reidel), p. 143.
 Merrill, K. M. 1977, in *IAU Colloquium 42, The Interaction of Variable Stars with Their Environment*, ed. R. Kippenhahn, J. Rake, and W. Strohmeier (*Veröff. Remeis-Sternw. Bamberg*, Vol. **11**, No. 121), p. 446.
 Peimbert, M., Torres-Peimbert, S., and Rayo, J. F. 1978, *Ap. J.*, **220**, 516.
 Puetter, R. C., Russell, R. W., Soifer, B. T., and Willner, S. P. 1979, *Ap. J.*, **228**, 118.
 Reifenstein, E. C., III, Wilson, T. L., Burke, B. F., Mezger, P. G., and Altenhoff, W. J. 1970, *Astr. Ap.*, **4**, 357.
 Rossano, G. S., and Russell, R. W. 1981, *Ap. J.*, **250**, 227.
 Russell, R. W., Soifer, B. T., and Willner, S. P. 1977, *Ap. J. (Letters)*, **217**, L149.
 Shaver, P. A., McGee, R. X., Newton, L. M., Danks, A. C., and Pottash, S. R. 1983, *M.N.R.A.S.*, **204**, 53.
 Talent, P. L., and Dufour, R. J. 1979, *Ap. J.*, **233**, 888.
 Thackeray, A. D. 1950, *M.N.R.A.S.*, **110**, 343.
 Thronson, H. A., Jr., Loewenstein, R. F., and Stokes, G. M. 1979, *A.J.*, **84**, 1328.
 Turner, B. E., Balick, B., Cudaback, D. D., Heiles, C., and Boyle, R. J. 1974, *Ap. J.*, **194**, 279.
 Wink, J. E., Altenhoff, W. J., and Webster, W. J., Jr. 1975, *Astr. Ap.*, **38**, 109.
 Woodward, C. E., Pipher, J. L., Helfer, H. L., Sharpless, S., Lacasse, M., Herter, T., and Willner, S. P. 1984, in preparation.
 Woolf, N. J. 1961, *Pub. A.S.P.*, **73**, 206.
 Wright, E. L., Lada, C. J., Fazio, G. G., Kleinmann, D. E., and Low, F. J. 1977, *A.J.*, **82**, 132.
 Wynn-Williams, C. G., Downes, D., and Wilson, T. L. 1971, *Ap. Letters*, **9**, 113.
 Zeilik, M., II. 1979, *A.J.*, **84**, 341.
 Zeilik, M., II, and Heckert, P. A. 1977, *A.J.*, **82**, 824.
 Zeilik, M., II, Kleinmann, D. E., and Wright, E. L. 1975, *Ap. J.*, **119**, 401.

D. A. BRIOTTA, JR., and J. R. HOUCK: Cornell University, Department of Astronomy, Space Science Building, Ithaca, NY 14853

H. L. HELFER and J. L. PIPHER: University of Rochester, Department of Physics and Astronomy, Rochester, NY 14627

T. HERTER: Grumman Aerospace Corporation Plant 26, Bethpage, NY 11714

B. JONES: Center for Astrophysics and Space Science, University of California at San Diego, C-011, La Jolla, CA 92093

S. P. WILLNER: Harvard-Smithsonian Center for Astrophysics, 60 Garden Street, Cambridge, MA 02138